

Review

A Review of Simulation Models of Heat Extraction for a Geothermal Reservoir in an Enhanced Geothermal System

Xiang Gao, Tailu Li ^{*}, Yao Zhang, Xiangfei Kong  and Nan Meng

School of Energy and Environmental Engineering, Hebei University of Technology, Tianjin 400301, China

^{*} Correspondence: 2018020@hebut.edu.cn; Tel./Fax: +86-22-60435787

Abstract: This paper reviews the heat transfer model for geothermal reservoirs, the fracture network in reservoirs, and the numerical model of hydraulic fracturing. The first section reviews the heat transfer models, which contain the single-porosity model, the dual-porosity model, and the multi-porosity model; meanwhile the mathematical equations of the porosity model are summarized. Then, this paper introduces the fracture network model in reservoirs and the numerical method of computational heat transfer. In the second section, on the basis of the conventional fracture theory, the PKN (Perkins–Kern–Nordgren) model and KGD (Khristianovic–Geertsma–De Klerk) model are reviewed. Meanwhile, the DFN (discrete fracture network) model, P3D (pseudo-3D) model, and PL3D (planar 3D) model are reviewed. The results show that the stimulated reservoir volume method has advantages in describing the fracture network. However, stimulated reservoir volume methods need more computational resources than conventional fracture methods. The third section reviews the numerical models of hydraulic fracturing, which contains the finite element method (FEM), the discrete element method (DEM), and the boundary element method (BEM). The comparison of these methods shows that the FEM can reduce the computational resources when calculating the fluid flow, heat transfer and fracture propagations in a reservoir. Thus, a mature model for geothermal reservoirs can be developed by coupling the processes of heat transfer, fluid flow and fracture propagation.

Keywords: hot dry rock; porosity model; fracture network; hydraulic fracturing; numerical model



Citation: Gao, X.; Li, T.; Zhang, Y.; Kong, X.; Meng, N. A Review of Simulation Models of Heat Extraction for a Geothermal Reservoir in an Enhanced Geothermal System. *Energies* **2022**, *15*, 7148. <https://doi.org/10.3390/en15197148>

Academic Editor: Carlo Roselli

Received: 1 September 2022

Accepted: 25 September 2022

Published: 28 September 2022

Publisher's Note: MDPI stays neutral with regard to jurisdictional claims in published maps and institutional affiliations.



Copyright: © 2022 by the authors. Licensee MDPI, Basel, Switzerland. This article is an open access article distributed under the terms and conditions of the Creative Commons Attribution (CC BY) license (<https://creativecommons.org/licenses/by/4.0/>).

1. Introduction

In recent years, CO₂ emissions from human industrial activity have aggravated climate change. However, the energy source of human industrial activity mainly originates from fossil fuels. Thus, an effective approach to weaken CO₂ emissions is that conventional fossil fuels are replaced by the utilization of renewable energy.

On the basis of statistics of geothermal resources, there are 118 EJ/year at a depth of up to 3 km and 1109 EJ/year to a depth of 10 km [1–4]. The geothermal system can be divided into hydrothermal systems and enhanced geothermal systems according to the characteristics of underground rock. For hydrothermal systems, the main characteristics of underground rocks are their high permeability and that groundwater is generally presented underground, while the enhanced geothermal system extracts the heat from the hot dry rock to generate power. Hot dry rock has low permeability, and there is no groundwater underground within this depth range. When compared with the hydrothermal system, the enhanced geothermal system can acquire more heat in artificial fractures. The main processes of the construction include: (1) exploration of hot dry rock; (2) investigation of fracture distribution; (3) constructing an injection and production well; (4) implementation of hydraulic fracturing technology for producing a geothermal reservoir; (5) closed loop of injection wells, production wells, and reservoir; (6) implementation of power generation [5–8]. An enhanced geothermal system is shown as Figure 1. Thus, other than the permeability and the characteristics of hot dry rock, an enhanced geothermal system is

similar to a hydrothermal system. The investigation of the geothermal reservoir model is the critical issue for enhanced geothermal systems.

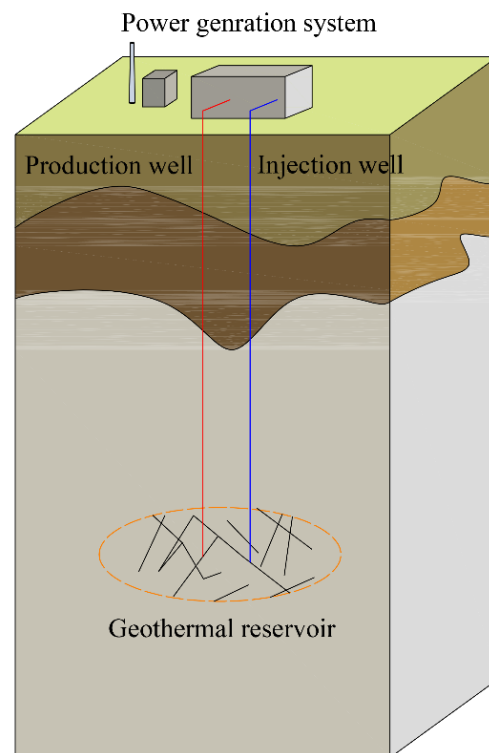


Figure 1. Schematic diagram of enhanced geothermal reservoir.

Currently, many countries have developed enhanced geothermal systems.

According to the sustainable development scenario globally, geothermal capacity additions have averaged 500 MW per year in the last five years by the year 2020 [9]. The trend is shown in Figure 2. In Figure 2, emerging economies have the most growth in the world; this is because there is still a large number of untapped geothermal resource availability. Based on IEA statistics, if the target for renewable energy usage is set as the sustainable development scenario level, the capacity of power generation from geothermal resources will maintain a growth rate of 10% per year before 2030. Thus, there is a large potential to develop enhanced geothermal systems.

The first experimental site of an enhanced geothermal system is located in New Mexico, named Fenton Hill [10–12]. This projection verified the feasibility of enhanced geothermal systems in 1974; meanwhile, this deep geothermal resource is named as hot dry rock [13]. During this period of development, the key technologies were originated by the oil or gas industry. Relying on this method, a series of projects were implemented, such as Fenton Hill, Rosemanowes, Hijori, Fjällbacka, and Ogachi site [14–18]. On the basis of the statistics over the past years, the local conditions of each site determine the performance of the enhanced geothermal system. Thus, the US government divides the developed technologies into three categories: in-field enhanced geothermal system, near-field enhanced geothermal system and greenfield enhanced geothermal system. For the early sites, most of the sites belong to the greenfield enhanced geothermal system category. More information on the developments of sites can be reviewed in the references.

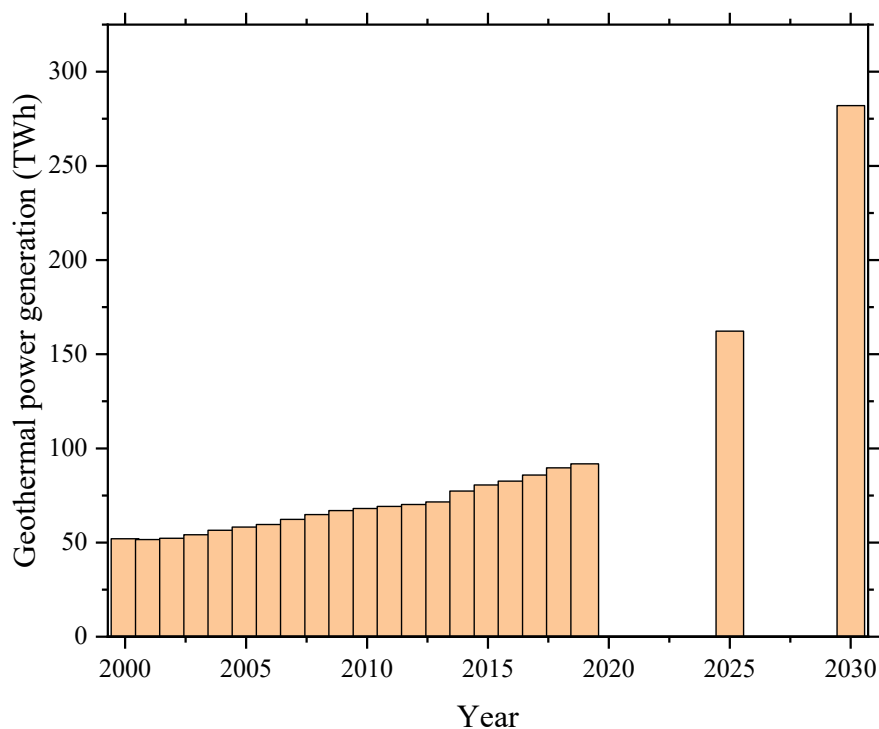


Figure 2. Trend of the installed capacity of geothermal power generation.

On the basis of the above experimental projects, the high cost of experiments limits their implementation in many countries, but the numerical simulation has the advantage of investigation in different conditions with a low cost [19]. A completely numerical model includes three parts: the power generation system, the numerical model of injection and production wells, and a geothermal reservoir [20–22]. The heat transfer in the geothermal reservoir determines the performance of the entire system; meanwhile, the fracture distribution and the mathematical description can directly impact the results of numerical simulation in geothermal reservoirs [23–25]. Therefore, this paper mainly compared the different fracture model, numerical model of hydraulic fracturing, and the models of fracture reservoir for an enhanced geothermal system. According to the introduction of these different models, the characteristics, or the advantage/disadvantage of heat transfer in reservoirs, were analyzed. Firstly, we review the common model of enhanced geothermal systems based on the porous media model in Section 2. Then, the conventional fracture theory method and stimulated reservoir volume method are reviewed in Section 3. The different numerical models of hydraulic fracturing are compared and reviewed in Section 4. At last, a general model for a geothermal reservoir in EGS is summarized in Section 5.

2. The Applications of Enhanced Geothermal System in Porosity Models

If an enhanced geothermal reservoir is implemented successfully, there will be two critical issues for enhanced geothermal system power plant development. First, effective heat transfer fractures with large volume, high porosity, high permeability, and high hydraulic conductivity are formed in the reservoir. The second is to successfully extract the heat from the reservoir for power generation. Both crucial issues are determined by the heat transfer in the geothermal reservoir. A geothermal reservoir consists of fracture and hot dry rock at a depth from 3 km to 10 km, and the porosity model is generally employed to establish the numerical model. The porosity model can be divided into three types according to the characteristics of the fracture network: the single-porosity model, the dual-porosity model, and the multi-porosity model [26–31]. The single-porosity model assumes the geothermal reservoir as a homogeneous porous medium, thus, the detailed characteristics of fracture (hydraulic conductivity, fracture distribution, and the fracture

structure) are neglected; only the porosity is used as the characteristic parameter for the geothermal reservoir. Thus, porosity in the single-porosity model is obtained by average or approximation [32]. In this section, the single-porosity models, dual-porosity models, and multi-porosity models in enhanced geothermal systems are reviewed.

2.1. The Single-Porosity Model

In the single-porosity model, the geothermal reservoir is regarded as the single porosity region to solve the fluid flow and heat transfer between hot dry rock and a fracture. Jiang et al. [33] used the single-porosity model to establish the numerical model of geothermal reservoirs. The numerical calculation region of a geothermal reservoir is treated as the an equivalent porous medium with a single porosity. Thus, the whole model of the geothermal reservoir is introduced in the framing of the porous media model. To maintain the high computational efficiency, the originated calculation region is divided into different sub-regions for numerical calculation. Thus, the assumption of local thermal non-equilibrium is employed to describe the heat transfer between the hot dry rock and fracture. The temperature in the apertures of fractures is not equal to the temperature of hot dry rock. The numerical results showed that this method has matched boundary conditions between sub-regions in traditional multi-domain methods. However, the numerical model of geothermal reservoirs based on the single-porosity model divides the single regions into three subregions for numerical simulation. Thus, the structure of fracture and fluid loss is neglected in the geothermal reservoir. This simplification loses the detailed description of the complex structure of fractures in the geothermal reservoir. This defect obstructs the application of the single-porosity model. Currently, fractures and hot dry rock in most papers can be described by the dual-porosity model for offsetting this disadvantage.

2.2. The Dual-Porosity Model

Single-porosity models are difficult to use to describe the complex fracture network [34–37] because the single-porosity region is assumed to represent the geothermal reservoir. To improve the single-porosity model, the dual-porosity model or the multi-porosity model is established to divide the geothermal reservoir into different sub-regions for numerical simulation. The dual-porosity model regards the geothermal reservoir as two different porous regions: the fracture network is described as a high-porosity region, and hot dry rock is treated as the low-porosity region.

The dual-porosity model was first established by Barenblatt et al. [38], and Warren et al. [39] investigated the flow behavior in fractured reservoirs with the dual-porosity model. To describe the transport of global fluid in a matrix, the dual-porosity and dual-permeability model were combined to solve matrix-to-matrix and fracture-to-fracture flow [40]. During the early development of the dual-porosity model, it only involved the fluid flow without the heat transfer process. An idealized model was used for studying the characteristic behavior of a naturally fractured or vugular reservoir, which treated these parameters as porosity mediums [41]. To describe the transient flow in each matrix block, Multiple Interacting Continua (MINC) was employed to discretize the matrix blocks. For gravity segregation in individual matrix blocks, the “Subdomain” method was used to vertically discretize matrix block into vertically stacked sub-blocks to allow gravity drainage between them [42]. The dual-porosity model has less computational and conceptual demand, thus, this model has been widely used to calculate the heat transfer or fluid flow in the enhanced geothermal system. For instance, Zeng et al. [43] employed the typical dual-porosity model to establish the numerical model based on well DP23-1 at the Desert Peak geothermal field. Two horizontal wells were used to connect the cycle between the injection well and production well. In this study, local thermal equilibrium was employed to describe the temperature in different porous medium regions. The temperature of fluid in fractures, fractured surfaces, and hot dry rock were assumed as the same temperature, which equaled the temperature of the porous medium. Then, the numerical results were validated by the experimental results, so this approach provided an effective reference and

estimation for practical reservoir performance [44–47]. The main parameters of the study for DP32-1 site are shown in Table 1 and the location of the two horizontal wells in the geothermal reservoir is shown in Figure 3. As shown in Figure 3, this study employed the two horizontal wells to transfer heat between hot dry rock and fractures. The injected cold water flowed into the bottom horizontal well; after heat transfer with hot dry rock, the geothermal reservoir produced hot water, which flowed into the top horizontal wells for power generation. There was no water loss during the heat exchange in the geothermal reservoir. The result showed that the main parameters of heat transfer included the permeability of geothermal reservoir, production rate, and temperature of the injection well. Furthermore, the numerical simulation results proved that the accuracy meets the requirements well based on the Desert Peak experimental data.

Table 1. The Parameters of the DP32-1 Site [43].

The Development Zone	1610 m × 2606 m
target depth	1219 m to 2743 m
Hot dry rock temperature	between 207 °C and 216 °C; average value of 210 °C
porosity	2% (439 m investigation radius)
permeability	0.01 mD (439 m investigation radius)
reservoir depth	1219 m to 1619 m
pressure of reservoir	9.65 MPa to 13.10 MPa
fracture spacing	less than 2 m
reservoir domain	400 m × 400 m × 500 m
injection temperature	60 °C
bottomhole pressure of production well	5 MPa

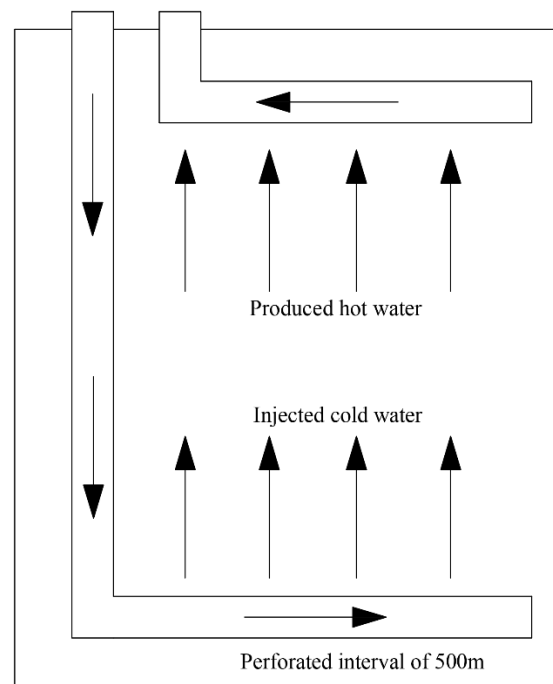


Figure 3. Structure of two horizontal wells in hot dry rock [43].

The above research only considered the fluid flow and heat transfer in geothermal reservoirs. However, heat extraction in geothermal reservoirs leads to the decrease of temperature; then, the stress distribution is changed with the increase of production time. Furthermore, the structure of a fracture will be changed under the variation of thermal stress. The permeability also has the variation along with the change of fracture. Thus, the coupled relationship between heat transfer, fluid flow and stress is one of the research trends. This coupled model of enhanced geothermal reservoirs is called the THM model

(thermal–hydrologic–mechanical). Due to the equation of hot dry rock determining the heat transfer between fluid flow and hot dry rock directly, thus, the governing equation of hot dry rock is a critical issue in the TH (thermal–hydrologic) model. There are various methods to describe the characteristic of rock matrix. Li et al. [48] used the porosity model to describe the geothermal reservoir with fractures. The constitutive relation of hot dry rock was assumed to obey the generalized Hooke’s law. To describe the fracture aperture, the fracture constitutive model (proposed by Li et al. [49]) was used to describe the change of the fracture aperture at shear, tensile and stress states; Cao et al. [50] also regarded hot dry rock as a linearly elastic solid, obeying the generalized Hooke’s law. This paper employed the mean total stress as the only primary variable for mechanical processes, meanwhile, the simplified treatment of rock deformation was obeyed by the relation of volumetric strain and mean normal stress. Samardzioska et al. [51] compared three different methods of fluid flow in fractured porous media, including discrete fracture/non-homogeneous, equivalent continuum, and dual-porosity models. The fracture/non-homogeneous model with a discrete fracture network assumed the fractured porous media as being an incompressible non-homogeneous media. The three approaches are shown in Figure 4.

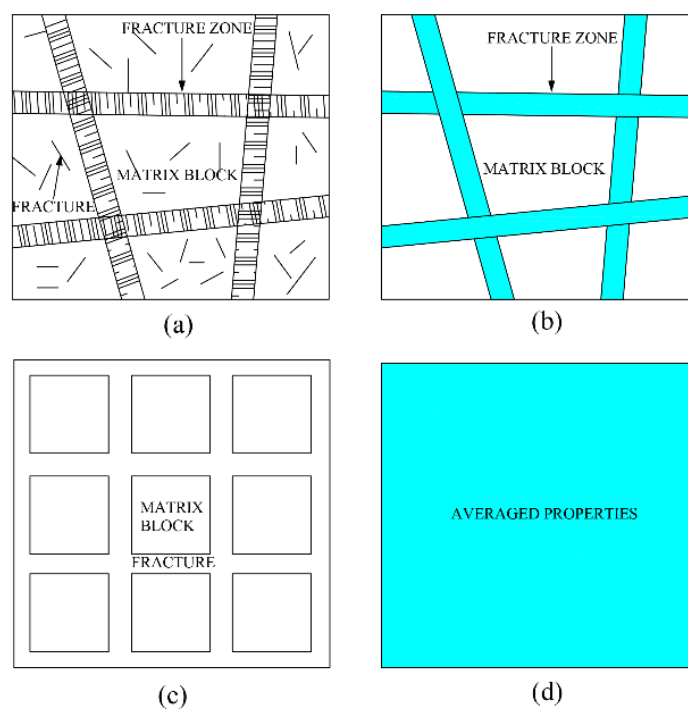


Figure 4. (a) Fractured porous media, (b) non-homogeneous representation, (c) dual porosity representation and (d) equivalent continuum representation [51].

In this model, only the finite fracture or fracture region was considered when the approach was applied. Based on an equivalent continuum medium, the difference from the non-homogeneous was that the fractured regions were regarded as a continuum medium with properties calculated by an averaging procedure. The results showed that when compared with the FEM–BEM (finite element method–boundary element method) approach, there was no coupling compatibility of the two models for the BE DRM–MD (boundary element dual reciprocity method–multi domain method) approach. However, this approach assumed that there is no distinction between the fractures and hot dry rock, therefore, when the fractured regions had reached a sufficiently large volume, it was impossible to obtain a correct estimate in a local point of the domain. Aimed at the dual-porosity models, this paper investigated the fluid flow between hot dry rock and a fracture network, and hot dry rock was considered a fully saturated porous medium. The results showed that the dual-porosity model occupied less computational resources than other models. As shown

in above numerical model, there are many complex models conceived for describing heat transfer in reservoirs [52].

On the basis of the above references, when a model is established to describe the behavior of fluid flow in the fracture and the heat transfer between fractures and matrix, most of the research is based on the Darcy's law for porosity media and Hooke's law for rock matrix in the THM model [53–55]. However, the Darcy's law is applicable under the condition of slow, viscous flow [56–58]. The fluid flow in reservoirs is so complex that the Darcy's law may be not applied in some conditions.

2.3. The Multi-Porosity Model

Although the dual-porosity model has been widely used to describe the geothermal reservoir, the inherent heterogeneity of hot dry rock limits the improvement of accuracy. On the basis of the porosity model, multi-porosity models can describe the primary fractures, the secondary fractures, faults, and micro-fractures; meanwhile, the hierarchical permeability structures or flow paths also can be introduced into this model. Currently, multi-porosity models are still in development. A triple-porosity model is the research focus. Musa D. et al. [36] established a triple-porosity model to represent the heterogeneity of naturally fractured–faulted geothermal reservoirs. On the basis of the Soultz graben formation, the geothermal reservoir was assumed as the porous medium with different regions, including the hot dry rock, faults and fractures. The heat transfer between different porous regions and geothermal fluid was described by the energy conservation equation and Fourier's constitutive relation. The result showed that the finite element method was in good agreement with the analytical solution. Zhao et al. [59] used the triple-porosity models to establish the numerical model of the gas within shale and the fractures stored in two statuses: adsorbed gas and free gas. This paper employed the analytical solution to solve the gas flow. The constitutive equation used the Laplace transformation to obtain the analytical solution. Huang et al. [60] established a multi-porosity model to describe the shale reservoir. Each matrix grid was divided on the basis of the experimental pore size data [61]. However, the application of multiple porous media in a shale reservoir lead to more uncertainties and complexities in the numerical simulation; thus, the computing resources will be significantly increased.

For the geothermal reservoir in an enhanced geothermal system, there are also other models describing the fluid flow and heat transfer in reservoirs, for instance, the equivalent pipe network model and stochastic continuum or fractured continuum model. The details for the equivalent pipe network model and stochastic continuum or fractured continuum mode can be overviewed in references [62–68] and references [48,55,69–74], respectively. Currently, most THM models employ the dual-porosity model to describe the heat transfer in geothermal reservoirs. The multi-porosity models are mostly employed to describe shale reservoirs or petroleum drilling. Due to the complex structure of fracture in geothermal reservoirs, the multi-porosity model divides the different characteristic of fracture and matrix (mainly considered permeability and porosity) into various multi-porosity regions. Meanwhile, a multi-porosity model can introduce the precipitation–dissolution reaction to simulate the geochemical processes in a geothermal reservoir, therefore, the porosity model has the potential to solve multi-physics fields for enhanced geothermal systems. Based on the characteristic of porosity models, there are a few features as follows:

1. The combination between the multi-porosity model and fracture network in geothermal reservoirs has received extensive attention currently, however, the original intention of the porosity model is to simplify the complicated fracture network; thus, this combination has again complicated the geothermal reservoir. This is mainly due to the improvement of computer computing performance. Due to some parameters in porosity models with statistical features, the selection of these parameters values is the key issue in the establishment of numerical simulations. The parameters with statistical features are not simply equal to the actual experimental value for geothermal reservoirs.

2. Porosity models have neglected many characteristics of geothermal reservoirs, so it is difficult to explain a given heat transfer or fluid flow in a geothermal reservoir unless the N-S equation is employed. Porosity models are more applicable in engineering fields.
3. How to make actual distribution of fracture in geothermal reservoir equivalent into the numerical model is the key factor for numerical simulation.

3. The Numerical Model for Fracture Networks in a Reservoir

Currently, there are two theories of induced fractures for the petroleum or gas industry: the conventional fracture theory based on linear elastic mechanics and the volume-fracturing method. For the conventional fracture theory, the rock is assumed as being a homogeneous medium [75]. The induced fracture is caused by the tensile failure of a fracture and is perpendicular to the minimum in situ horizontal stress [76,77]. However, the theory only considers the physical dimension and fracture-induced direction of the hydraulic fracture. Although various extensions of this method have been developed by this theory, it is difficult to accurately describe the extension and geometry of the hydraulic fracture. On the contrary, the volume-fracturing theory abandons the assumption of conventional fracture theory. The reservoir characteristic factors that determine whether the reservoir can achieve volume fracturing mainly include rock mineral composition, rock brittleness index, natural fracture development status and in situ stress conditions. Volume fracturing can generate secondary fractures in the side direction of the primary fracture. Then, a multistage fracture is generated in the side direction of the secondary fracture. Eventually, a fracture network is composed by these fractures. Thus, this theory can describe the generation of a complex fracture network.

3.1. Conventional Fracture Theory

The conventional fracture theory can be traced back to World War II for solving welding and wing designs [78]. During this period, rock fractures received much research attention. According to the different assumptions of fracture extension direction and height, there are two conventional fracture theories to describe the major fracture.

The PKN (Perkins–Kern–Nordgren) model was established by three contributing researchers (Perkin, Kerns, and Nordgren). Currently, the PKN model is one of the most widely used hydraulic fracture models for the oil and gas reservoirs [78]. For the PKN model, also called the blade-shaped or finger-like model, the fracture length is assumed to be much greater than the fracture height, and the fracture width is calculated by a plane strain elasticity equation and a viscous fluid flow equation. However, the water loss between fracture and rock matrix are not considered. To solve the leak-off in reservoirs, Nordgren et al. [79] considered a one-dimensional model based on Carter's law to revise the Perkins and Kern's model for investigating water loss. The numerical model employed the nonlinear partial differential governing equations, which were solved by their analytical asymptotic solutions. Then, this paper investigated the two cases with leak-off and without leak-off. The classic PKN model had been completely established by the above processes. The original PKN model considers the turbulent effect, particle velocity approach, and fluid flux approach [80].

Another conventional theory is called the KGD (Khristianovic–Geertsma–De Klerk) model, which was established by Khristianovich and Zheltov in 1955 [81,82]. This model assumes that fracture height is equal to the reservoir height. The fracturing fluid flows only occurred along the direction of the fracture length under a one-dimensional assumption. In this model, viscous flow theory was employed to relate the mathematical model of the extension of fractures. For the effect of leak-off, the early KGD model introduced the rate of water loss per unit of the exposed fracture surface to show the fluid loss.

On the basis of above references about the PKN model and KGD model, there is a significant difference between the PKN and KGD model in the rectangular fracture section. The KGD model is appropriated for fracture lengths higher than the fracture height [83]. However, when one considers the vertical extension of the fracture, a three-dimensional

fracturing numerical simulation is needed to calculate the expansion of the height, width and length of fractures. For the conventional fracture theory, the PKN and KGD models are mainly on the basis of elastic mechanics with the assumptions of continuity, obeying Hooke's law, homogeneity, and isotropy for reservoirs. Thus, the conventional PKN or KGD models have limitations when a three-dimensional condition is considered. The two models cannot solve the vertical fracture extension. Currently, there are various revised methods based on the conventional fracture theory.

Based on these classical models, the numerical models, such as P3D, PL3D and Full 3D, were developed to describe the fracture height growth in reservoirs. For the P3D model, it was established in the 1980s based on the PKN model to investigate the extension of a vertical hydraulic fracture into a horizontally layered reservoir. In contrast to the PKN model, the height of the P3D fracture is not limited to the reservoirs thickness [82,84,85]. Adachi et al. [86] employed the P3D model as the numerical solution of the variation of the planar fracture in the elastic layers under different assumptions. These assumptions were as follows: water loss into the geothermal reservoir was treated on the basis of Carter's models; there was enough viscosity for filtrate to fully displace the fluid already present in the fracture aperture. In order to transform the mathematical model to a dimensionless form, the governing equation was expressed as the product of the characteristic quantities and dimension-less variables. Thus, this paper first adopted a continuous equation and scaling of the problem. A nonlinear convection diffusion equation with a delay term was employed to establish the mean fracture aperture. Since the discrete equations are implemented in MATLAB under code colP3D [86], this would provide an implementable design code for industry.

However, two questions need an answer when the P3D model is employed [87]. The first one is how to consistently grow the height in an arbitrary case. The second question is as follows: under which conditions does any extension of the P3D model become inapplicable? In order to solve the two questions, Linkov et al. [87] had established a P3D model in the MATLAB and Python environment. The study had solved the two questions by a combination of the original P3D model and KGD model. For the height growth, the original P3D model was improved by assigning an equal condition. Through the comparison of the bench-mark solution [88], the revised P3D model can be used to contrast arbitrary stresses, including the cases of zero and negative contrasts. However, the speed of the height growth was needed to be identified to describe the extension of the fracture tip. This improved model developed a general correspondence principle between KGD models and the P3D model. Since the classical KGD model does not account for leak-off losses, this model only kept the water loss in the continuity equation. Thus, the leak-off loss needed a further investigation. Yang et al. [89] investigated a novel P3D multi-cluster fracturing model to promote multiple-fracture uniform growth by numerical simulations. Since the previous pseudo-3D models [84,90,91] only considered net pressure and fracture toughness for fracture height, each propagation rate of fracture tip was simulated by its energy release rate [92]. In this study, there were various factors considered: the complex distributions of stress interactions between the fractures, in situ stresses, fracturing fluid leak-off, and fluid dynamic flow distributions into different fractures.

Due to the limitation of the classical P3D model with fracture extension in an impermeable region, there were two dissipative mechanisms that control the fracture extension: the energy release and the viscous dissipation when a new fracture surface was formed. In the classical P3D model, the fracture toughness in the lateral direction was not considered, while the fracture was only propagated in the viscous medium in the horizontal direction. Therefore, if the length of the fracture is nearly zero, the vertical height growth will be overestimated [88]. In order to revise the classical P3D mode, Dontsov et al. [88] employed the viscous height growth to correct the P3D model. For the revised model, it had neglected the inclination of the fracture footprint located within the stress barrier. Thus, each vertical section of a fracture in P3D model can be assumed as a KGD fracture. Currently, the P3D model has been corrected by various methods to increase the accuracy and calculation

efficiency. On the basis of the above references, the P3D model can be divided to cell-based or lumped approach [93]. Therefore, this model is widely employed to describe the single fracture growth in oil or gas reservoirs. For heat transfer between fractures and matrix (hot dry rock), P3D model can be introduced to solve the fluid flow in multiple layers. Currently, this model has replaced the PKN or KGD model in the oil or gas industry when a fracture network is described.

To improve the accuracy of numerical simulations, PL3D models consider the full 3D elasticity equations to describe the width of fractures. However, these models obviously demand more computational resources than P3D models. Thus, PL3D has not been widely employed in numerical simulations currently. In order to compare the above models, the detailed characteristics of models are shown as follows. The one-dimensional classical PKN model is propagated along the direction of the x -axis and is contained in a horizontal layer with an elliptical vertical cross-section and a constant height h . Thus, the region of fracturing is developed within h . For the constant height, the above references also have employed various methods for their revision, and more methods can be found in references [94–97]. The structure of this model is shown in Figure 5.

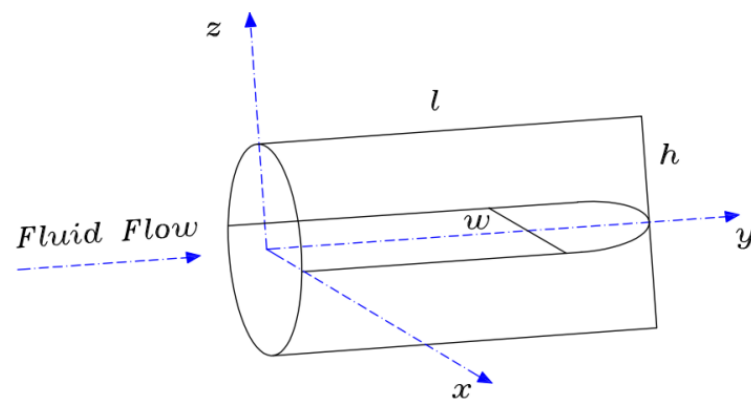


Figure 5. Structure of the PKN model of a hydraulic fracture: y -axis is the direction of fracture extension, w is the width of fracture, l is the length of fracture, and h is the height of fracture.

The KGD model assumes two simple propagation models for the fracture extension: the radially symmetrical extension caused by a point source and rectilinear propagation originating from a line source. For the fracture width, the model employs the elasticity theory to describe the width of fractures and an arbitrary normal stress. The significant characteristic of the KGD models is that the linearly expanding fractures are assumed to possess plane strain conditions, and the height of the fracture is not assumed as constant. The structure of the KGD methods is shown in Figure 6.

The P3D model is based on the PKN model and builds on the similar basic assumption such as continuity, isotropy, homogeneity, and obeying the Hooke's law. The P3D fracture is shown in Figure 7. The cell-based and lumped approach for P3D model is shown in Figures 8 and 9. For the fracture height in reservoirs, both P3D and PKN models treat the height as a constant over all layers. This model extends the PKN models to solve the multi-layer reservoir. However, P3D models still have difficulty in describing specific types of fractures. For instance, when there is a non-monotonic relationship between the layer confining stresses and the function of depth, or when unconfined height growth occurs, the P3D model tends to diverge numerically [93].

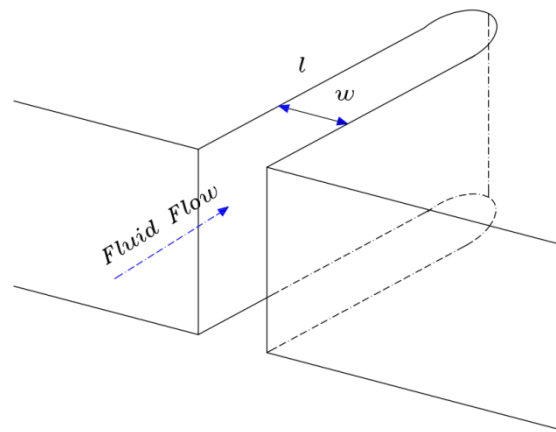


Figure 6. Structure of the KGD fracture extension in a hydraulic fracture: l is the length of fracture and w is the width of fracture.

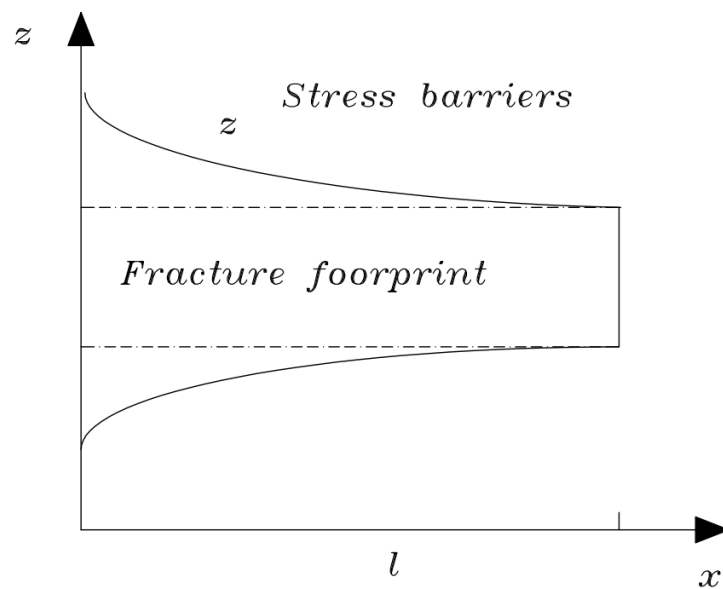


Figure 7. Schematics of the P3D fracture: x -axis is the direction of fracture extension; l is the length of fracture and z -axis is the height direction of fracture extension.

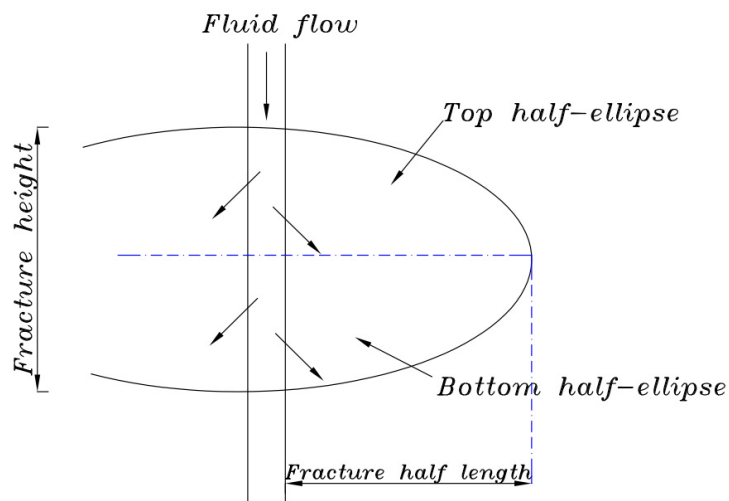


Figure 8. Schematic of fracture geometry on the basis of P3D model: the direction of fracture is perpendicular to the direction of fluid flow with an ellipse range.

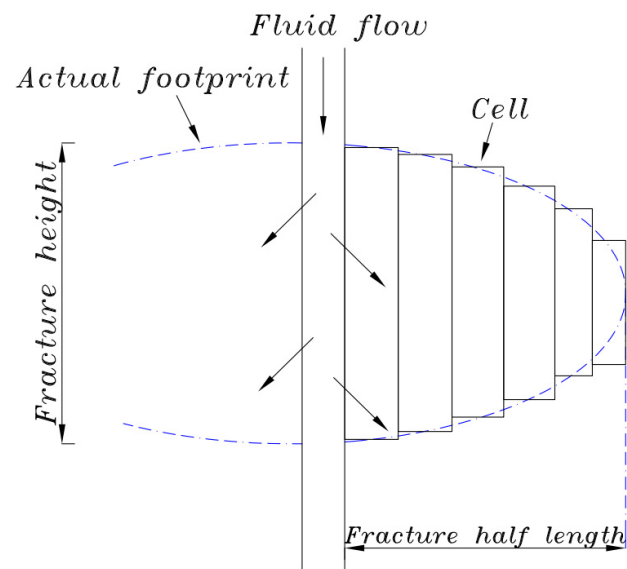


Figure 9. Schematic of cell-based P3D fracture extension: the fracture extension range is divided into multiple rectangles within the range of an ellipse.

For the reservoirs in the oil or gas industry, the constitutive equation based on a hydraulic fracturing model contains the fluid flow equation, the elasticity equation, the leak-off term, the proppant transport equation, and the fracture growth condition. All the equations also couple together to generate the solution of the fracture tip, the pressure of fluid, the width of the fracture, and the proppant concentration [93]. These equations are mainly introduced to solve the fluid flow in the various structure of the oil or gas reservoirs. The heat transfer process is not considered in these models in general. However, an enhanced geothermal system is mainly designed to extract heat from the geothermal reservoir to generate power. The heat transfer has a significant influence on the performance of a system. In addition, the fluid flow in reservoirs mainly employs the porous medium equation to describe the complex heat transfer and fluid flow. Although the porosity model reduces the computing resources to resolve the fluid flow and heat transfer, this model neglects the details for the two processes. Thus, if a fundamental study of heat transfer in geothermal reservoirs is investigated, the currently porosity media theory cannot provide the effective measures to understand the mechanism of fracturing. On the other hand, for the oil or gas reservoirs, the fluid flow and structure of the reservoirs can be appropriately described by various models such as the KGD model, PKN model, the P3D models, and the PL3D models. However, these models rarely take account heat transfer in reservoirs; there is no mature models to accurately describe the extension of fracture in geothermal reservoirs. Therefore, on the basis of oil or gas reservoirs and hot dry rock reservoirs, there is a contradiction between the two kinds of reservoirs: the conventional model for oil or gas reservoirs can accurately describe the fluid flow in reservoirs but heat transfer has difficulty in being taken into account, while the porous media model for the geothermal reservoirs can describe the heat transfer and fluid flow but cannot provide detailed characteristics to help in understanding the fundamental mechanism of heat transfer and fluid flow.

3.2. Stimulated Reservoir Volume

In the oil or gas industry, the early mining mode further expanded the multi-fracture along the primary fracture. Thus, the convention fracture theory had a great development in this period. However, with the depletion of an oil or gas reservoir, this mining mode cannot provide enough capacity for demands. Thus, stimulated reservoir volume technology was developed to increase production. This technology uses a hydraulic fracturing method to generate shear slip along a primary fracture for obtaining a micro-fracture, resulting in a fracture network to connect the entire reservoir. This technique was later applied to

EGS. Obviously, the conventional fracture theory can only solve the single fracture extension in a reservoir. However, there are many fractures in a geothermal reservoir, and thus the conventional fracture theory is not applicable in this case. A geothermal reservoir with a single fracture leads to a large deviation when compared with the actual geological condition. In order to solve this problem, some researchers introduce probability theory to describe the complex fracture distribution based on the equivalence principle. On the basis of this approach, the most widely used model is the DFN (discrete fracture network) model.

The DFN (discrete fracture network) model is a mature method to simulate the complex fractures in reservoirs. This model can employ the discrete method to explicitly describe each fracture in the domain and different cases of heat extraction from fractured formations [98,99]. For example, the distribution of fractures is calculated by the Monte-Carlo stochastic method. Through the comparison between the numerical result and experimental result, the real fracture distribution can be expressed as the equivalent to the numerical model based on the Monte-Carlo stochastic method. Therefore, this model makes up for the disadvantage of conventional fracture theory. According to this approach, the mechanic mechanism in geothermal reservoirs can be investigated. Salimzadeh et al. [100] investigated a strongly coupled THM model to simulate the geothermal extraction from an enhanced geothermal system with 3D DFN models. This study accounted for the hydraulic, mechanical, and thermal sub-models in the coupling algorithm. Because of the complexity of flow fluid, the pipe-network method (UPM) was employed to calculate the fluid flow in geothermal reservoirs. On the basis of the 20 years of modeling the geothermal extraction for the Habanero EGS reservoir, the proposed model was verified to be robust and effective for the THM-coupled process in three-dimensional fractured reservoirs. For the mesh generation in thermal/hydraulic and mechanical simulations, this study used the mesh methods established by Wang et al. [101], which had the most considerable computational intensity.

For a natural fracture network, a DNF model can be established from stochastic realization, geological mapping, or geomechanical simulation [102]. Currently, the geologically mapped fracture networks were employed to represent the generation of fractures [103]. However, this model was mainly constrained to 2D analysis, while three-dimensional maps of large-scale geological structures may neglect some detailed characteristics such as the segmentation of faults, as well as impede the detection of small cracks widely spreading in hot dry rock. In order to resolve the generation of a completed 3D natural fracture systems, the stochastically generated fracture networks were developed in 1980s to study the fluid flow in complex fracture networks. This approach was based on two-dimensional or three-dimensional networks and treated the frequency, position, size, aperture and orientation as independent random variables to generate the fracture networks. However, due to the independence of these variables, there were large uncertainties for the generated fracture networks. The DFN model cannot guarantee consistency with the same group of parameters. Currently, several improvement methods have been developed. For instance, on the basis of the development of the geological history and the formation mechanism behind field observations of natural fracture systems [104–107], the linear elastic mechanics in fractures were introduced to simulate the geomechanically grown fracture networks [102,108]. In this approach, the extension of fractures obeyed a growth criterion, which contained the stress corrosion and stress intensity factor. For the two parameters, the analytical solutions, the boundary element method, or finite element method can be used to calculate them. Thus, this model had the advantage of combining the geometry and topology of fracture networks. However, due to the complexity of the real natural fractures, there was still difficulty and uncertainly when coupled hydrological, tectonic, chemical, and thermal processes were considered [102,109,110]. For more detailed overviews of improvements, there are several references that overview the specific approaches [111–113].

On the basis of the above references for the DFN model, multi-fractures can be used to describe the fluid flow in a reservoir. The conventional models such as the P3D and PL3D model are limited to represent one fracture located in a single vertical plane, therefore, the DFN model has a greater advantage than conventional fracture theory when the fluid flow

is investigated. However, for the geothermal reservoirs, there is no appropriate heat transfer model to describe this discrete fracture network. Currently, some works only simplified the fracture as a rectangular channel to investigate the heat transfer between the rock and fracture network [114]. Since the DFN model has occupied massive computing resources when a fluid flow in a three-dimensional case is considered, this approach will expand the footprint of computing resources. Besides, since the porosity model has proven the accuracy of numerical simulations of heat transfer in reservoirs, some of the characteristics of reservoirs may be appropriately substituted to the permeability and porosity variables in the porosity model if the reservoirs are mainly considered in terms of the heat transfer. The main reason is that heat transfer directly impacts the performance of power generation in enhanced geothermal systems. The DFN model employs the statistical methods to represent the characteristic of fractures. Such an accurate discrete fracture network can be replaced by an equivalent permeability and porosity to resolve the heat transfer under the sufficient accuracy.

4. The Numerical Model of Hydraulic Fracturing

For the above theory of fracture growth and fluid flow, there are various numerical simulation solution methods for solving these nonlinear partial differential equations, such as finite element method (FEM), discrete element method (DEM), and the boundary element method (BEM) [115,116]. For the enhanced geothermal system, the approaches which are employed in oil or gas reservoirs can be generalized to hot dry rock reservoirs. The above numerical simulation solution also can be introduced to solve the similar nonlinear partial differential equations in enhanced geothermal system.

When a model employs the FEM (finite element method), the first step is that the computational domain is divided into a series of elements, then, some point is selected as the node in each element. Then, the discrete equations are acquired by integrating for governing equations. Before the integration of the governing equation, a shape function and a weight function are used to substitute into the governing equation. Therefore, a series of algebraic equation sets are obtained in a node. Thus, the finite element method has an advantage to solve the irregular computational domain. Based on the finite element method, the key issue is the form of shape function. Currently, there are various approaches to construct the shape function, such as in references [117,118]. Since this method can describe the hot dry rock and fracture with the same nodes, the method may have more potential to solve the complex heat transfer between fracture and hot dry rock compared other numerical solution.

DEM (discrete element method) has been widely employed in numerical simulations of hydraulic fracturing. This method treats the rock matrix as a discrete rigid block. For each interconnected rigid block, an explicit difference scheme is used to simulate the extension. Besides, the fracture between discrete blocks allows the fluid flow, therefore, discrete element method can calculate the coupled fluid–structure interaction in fractures. Liu et al. [119] employed the DEM to investigate the fluid-mechanical coupling in a gas reservoir. They used the numerical simulation to calculate the relationships between hydraulic crack initiation pressure, expansion speed, stress wave frequency, maximum principal stress and failure mode. The results showed that the fracture generation deflected towards the direction of the wave transmission. Ghaderi et al. [120] studied the hydraulic fracture generation by DEM and XFEM (extended finite element method). In this paper, they represented the propagation of hydraulic fractures along the natural fracture network with DEM and described the interaction between the natural and induced fractures by using XFEM. For the extended finite element, this model only required the description of geometrical domain without remeshing. The results showed that the two methods can examine the effect of the length of an induced fracture on the production rate in naturally fractured regions and the deformation of natural fractures. This paper generated the hydraulic fractures model via the distinct element method and introduced the extended finite element method to calculate the interaction between the natural and induced fractures.

The combined model proved its feasibility by other numerical simulations. Currently, this method only considers the interaction of the induced and natural fractures; the complex fluid flow and heat transfer are not considered. Thus, there is potential to further the implementation in geothermal reservoirs.

The BEM (boundary element method) is another numerical method widely used in fracture propagation simulation. The BEM only discretizes the boundary and fracture surfaces for its calculation. Therefore, this model costs less computational time and resources when generating new elements in fracture growth. Furthermore, the BEM has been considered as accurate in fracture growth, especially when mixed mode fracture propagation is taken into account [121,122]. To improve the efficiency and accuracy in this model, Crouch et al. [123] employed the displacement discontinuity method and Green's functions to revise the BEM. For multiple fracture propagation, various BEM models were introduced in the paper. Multiple crack-hole interactions [124,125] and multiple crack interactions had been successfully employed. However, these models neglected the coalescence and localization phenomena. Leonel et al. [126] developed a two-dimensional BEM model to investigate multiple random fracture generation in brittle materials. In this study, they employed the dual boundary element formulation to analyze arbitrary fracture growth. After the verification of three examples of multiple and simple fracture propagation, the results showed that this approach provides a reference to model multiple fracture growths in the two-dimensional structures.

The recent references of the above numerical model are displayed at Table 2.

Table 2. Some numerical models of hydraulic fracturing.

Method	Reference	Introduction
FEM	Wang et al. [127]	a 3D homogeneous and isotropic medium with hydraulic fracture and cemented natural fractures
FEM	Sun et al. [128]	a 3D-fractured porous media
FEM	Khoei et al. [129]	A cohesive crack model for nonlinear fracturing process occurring ahead of hydro-fracture tip
XFEM	Vahab et al. [130]	Hydro-fracture interaction scenarios with idealized naturally cemented faults
XFEM	Zhou et al. [131]	a 2D medium with hydraulic fracture and natural fractures
DEM	Huang et al. [132]	2D discrete element modeling was used to investigate the influence of the stiffness and toughness ratio
DEM	Zeng et al. [133]	The coupled CFD–DEM method was applied for proppant transport simulation
DEM	Jiao et al. [134]	A comprehensive THM coupling scheme was conducted in the LBM–DEM
DEM and XFEM	Ghaderi et al. [120]	Comparison between DEM and XFEM
BEM	Zhao et al. [135]	The BEM was applied in off-centered fractured vertical wells
BEM	Chen et al. [136]	Comparison between BEM and FVM
BEM	Xu et al. [137]	A semi-analytical solution of finite-conductivity MFHWs was established and solved by boundary element method

For the heat transfer in reservoirs, there are various numerical methods for governing equations. The main methods conclude the finite difference method, the finite volume method, the finite element method, and the finite analytic method. In these methods, the finite volume method is the most widely used in the description of heat transfer. This method divides the computational domain into series of control volumes. For each control volume, the nodes are represented the control volumes, and the control volumes are integrated by conserving governing equations. For the finite difference method, this method is the earliest and the simplest approach used to calculate the fluid flow and heat transfer. The computational domain is divided into a series of points of intersection by grid lines. For each point of intersection, the Taylor expansion is used to generate the algebraic equation that is used to calculate the numerical solution. For the finite analytic method, this method used similar grid lines to divide the computational domain. The different

characteristic for the finite analytic method is that the nonlinear term in the governing equation is converted into local linearization form.

For a numerical simulation of geothermal reservoirs, FEM has been widely employed to solve the geothermal reservoir in CFD commercial software. This is because a CFD commercial software must consider the generality of the numerical method when it encounters different scenes. There may be other numerical methods suitable for solving geothermal reservoirs. Besides, if the THM model is used to describe the geothermal reservoir, the unstructured dynamic grid is needed to solve the expand of fracture width. Thus, the required computing resources will increase with the improvement of the number and complexity of fractures. Currently, the geothermal reservoir has no perfect approach which can balance the solution of heat transfer, fluid flow, fracture mechanics and geochemistry.

5. General Models for Geothermal Reservoir in EGS

Currently, with the development of exploration technology, the detailed geological conditions of the target layer have been easier to obtain. The combination between geothermal reservoirs and hydraulic fractures has become one of the research trends. Thus, in this section, a general model for a geothermal reservoir and hydraulic fracture in EGS is summarized on the basis of the porosity model.

5.1. Physical Model of Geothermal Reservoir and Hydraulic Fracture

Geothermal resource exploration is the first step to establish a physical model. Hot dry rock, as the geothermal heat source, is dominated by granite. Generally, granite is considered as an anisotropic medium with porosity of zero. After the hydraulic fracturing of such a medium, a fracture network is generated in the region of hot dry rock. According to the porous medium model, this geothermal reservoir can be considered as an anisotropic medium with a porosity of zero, and the fracture network is the only flow region of geothermal fluid.

5.2. Mathematical Model of Geothermal Reservoir Coupled with Hydraulic Fracture

According to the characteristics of physical models, the governing equation can be divided into a matrix (hot dry rock) and fracture.

Based on the porous medium model, unlike fluid mechanics, flow rate and density are not solved by continuity equations and momentum equations for the mechanics of flow through porous media. Generally, the momentum equation is replaced by Darcy's law to describe the seepage in a porous medium. For the convenience of engineering, Darcy's law is substituted into the continuity equation to compose the governing equation of seepage. With water as an example, the governing equation can be written as:

$$\frac{\partial(\phi\rho)}{\partial t} + \nabla \cdot (\rho\mathbf{V}) = 0 \quad (1)$$

$$\mathbf{V} = -\frac{\mathbf{K}}{\mu}\nabla p \quad (2)$$

where ρ is the density of geothermal fluid, ϕ is the porosity of the geothermal reservoir, \mathbf{K} is the permeability tensor, μ is the dynamic viscosity, p is the pressure of geothermal fluid, t is time, and \mathbf{V} is seepage velocity. In Equations (1) and (2), the gravity effect is neglected and there is no source term because there is no mass increase or decrease inside the local region of the geothermal reservoir.

Generally, water is considered as a slightly compressible fluid, thus, the state equation can be written as:

$$\rho = \rho_0[1 + c_f(p - p_0)] \quad (3)$$

$$\phi = \phi_0[1 + c_\phi(p - p_0)] \quad (4)$$

where c_f and c_ϕ is the compression factor.

Then, the seepage governing equation can be written as:

$$\phi\mu c \frac{\partial(p)}{\partial t} = \frac{\partial}{\partial x}(\mathbf{K}_x \frac{\partial p}{\partial x}) + \frac{\partial}{\partial y}(\mathbf{K}_y \frac{\partial p}{\partial y}) + \frac{\partial}{\partial z}(\mathbf{K}_z \frac{\partial p}{\partial z}) \quad (5)$$

where c is the system compressibility.

For the energy conservation equation, the fluid in the fracture and matrix (hot dry rock) can be written as Equations (6) and (7), respectively.

$$\phi(\rho c_p)_f \frac{\partial T}{\partial t} + (\rho c_p)_f (\mathbf{V} \cdot \nabla) T = \phi k_f \nabla^2 T + \phi q_f \quad (6)$$

$$(1-\phi)(\rho c_p)_s \frac{\partial T}{\partial t} = (1-\phi)k_f \nabla^2 T + (1-\phi)q_s \quad (7)$$

where subscripts f and s are the fluid and matrix, respectively.

5.3. Meshing, Discretization and Software

When the mathematical model has been established, meshing is needed to divide the calculated domain. If a fracture network is inserted into a geothermal reservoir, the discrete fracture network is generated according to Monte Carlo method. Thus, each grid will include the fracture and matrix. Then, according to the numerical method based on Section 4, the corresponding discrete equation is obtained by Equation (1) to Equation (7). Ultimately, the temperature and pressure field are obtained by the calculation of the discrete equation.

Currently, there is much commercial software for solving geothermal reservoir. Table 3 shows the characteristics of the used commercial software.

Table 3. Commercial software for solving geothermal reservoir.

Software	Characteristic
Ansys	Advantage of mesh generation, UDF can design the specific boundary and conditions.
Comsol	Suitable for coupling calculation of multiple physical fields, the corresponding modules has been integrated for geothermal reservoir.
Openfoam	Open-source software, support for custom programming.
TOUGH2	Good accuracy for the calculation of geothermal reservoir.

6. Conclusions

The enhanced geothermal system is a developing technology to extract the deep geothermal energy. The numerical simulation for the system includes the power generation system, vertical injection and production well model, and the geothermal reservoirs model. The main conclusion as follows:

1. On the basis of the comparison of different numerical models, the porosity model has an advantage when a model only considers the impact of heat transfer for the injection well and production well, but the complexity of fractures is difficult to represent based on the porosity model.
2. The selection of these parameters' values in the porosity model is the key issue in the establishment of numerical simulations. The parameters with statistical features are not simply equal to the actual experimental value for a geothermal reservoir.
3. For the fracture-generation technology, the stimulated reservoir volume technology has the more accuracy than conventional fracture theory when the multi-scale fracture propagations are described. The revised conventional fracture theory, such as in the P3D model, has introduced the high growth for a single fracture to describe the three-dimensional model of fracture propagation. Due to the stimulated reservoir volume technology based on the statistics data, this model can represent the characteristics of the geothermal reservoirs if the geological data are detailed.
4. After the comparison between different numerical models of hydraulic fracturing, since the finite element method can provide the same mesh and node for fracture propagation

and fluid flow in fracture, this model can reduce the computational time and resources. However, all numerical models need to be regenerated in the mesh to calculate the fracture propagation, and this step will occupy large computational resources.

5. The development technology for enhanced geothermal system is based on the experience of the oil or gas industry. In the oil or gas industry, the fluid flow in the reservoir is the main research focus. These mature numerical models have proven the effectiveness for fracture propagation and fluid flow. In contrast, the heat transfer is the most important factor for geothermal reservoirs, therefore, the numerical model for an enhanced geothermal system needs to include the heat transfer, fluid flow, and fracture propagation. Although the porosity model can calculate the heat transfer process to satisfy industrial demand, this equivalent model cannot provide the details of geothermal reservoirs. Thus, if a developed model based on the oil or gas industry contains the heat transfer process, this model can provide a precise description for geothermal reservoirs.

Funding: This research was funded by Postgraduate Innovation Funding Project of Hebei Province grant number No. CXZZBS2022029.

Acknowledgments: The authors are thankful to the anonymous reviewers for comments that helped us improve the paper content.

Conflicts of Interest: The authors declare no conflict of interest.

References

1. Haenel, R. Handbook of geothermal energy: By L.M. Edwards, G.V. Chilingar, H.H. Rieke III, W.H. Fertl (Editors). Gulf Publishing Company, Houston, 1982. (distr. in U.K. and W. Europe by MTP Press). ix + 613 pp., £56.25 (hardback). *J. Volcanol. Geoth. Res.* **1983**, *19*, 186–187. [[CrossRef](#)]
2. Zhou, D.; Tatomir, A.; Niemi, A.; Tsang, C.; Sauter, M. Study on the influence of randomly distributed fracture aperture in a fracture network on heat production from an enhanced geothermal system (EGS). *Energy* **2022**, *250*, 123781. [[CrossRef](#)]
3. Liu, G.; Zhou, C.; Rao, Z.; Liao, S. Impacts of fracture network geometries on numerical simulation and performance prediction of enhanced geothermal systems. *Renew. Energy* **2021**, *171*, 492–504. [[CrossRef](#)]
4. Zhang, B.; Qu, Z.; Guo, T.; Sheng, M.; Chen, M.; Wang, J.; Wang, Y.; Guo, C. Coupled thermal-hydraulic investigation on the heat extraction performance considering a fractal-like tree fracture network in a multilateral well enhanced geothermal system. *Appl. Therm. Eng.* **2022**, *208*, 118221. [[CrossRef](#)]
5. Xie, J.; Wang, J.; Liu, X. The role of fracture networks randomness in thermal utilization of enhanced geothermal system. *Int. Commun. Heat Mass Transf.* **2021**, *126*, 105414. [[CrossRef](#)]
6. Zheng, S.; Li, S.; Zhang, D. Fluid and heat flow in enhanced geothermal systems considering fracture geometrical and topological complexities: An extended embedded discrete fracture model. *Renew. Energy* **2021**, *179*, 163–178. [[CrossRef](#)]
7. Zhang, X.; Huang, Z.; Lei, Q.; Yao, J.; Gong, L.; Yang, W.; Yan, X.; Li, Y. Improving heat extraction performance of enhanced geothermal systems: Insights from critical fracture network parameter and multi-objective optimization method. *Appl. Therm. Eng.* **2022**, *213*, 118671. [[CrossRef](#)]
8. Li, L.; Guo, X.; Zhou, M.; Xiang, G.; Zhang, N.; Wang, Y.; Wang, S.; Pagou, A. The Investigation of Fracture Networks on Heat Extraction Performance for an Enhanced Geothermal System. *Energies* **2021**, *14*, 1635. [[CrossRef](#)]
9. IEA Renewables 2020. Available online: <https://www.iea.org/reports/renewables-2020> (accessed on 1 November 2020).
10. Gao, X.; Zhang, Y.; Huang, Y.; Ma, Y.; Zhao, Y.; Liu, Q. Study on heat extraction considering the number and orientation of multilateral wells in a complex fractured geothermal reservoir. *Renew. Energy* **2021**, *177*, 833–852. [[CrossRef](#)]
11. Rinaldi, A.P.; Rutqvist, J. Joint opening or hydroshearing? Analyzing a fracture zone stimulation at Fenton Hill. *Geothermics* **2019**, *77*, 83–98. [[CrossRef](#)]
12. Norbeck, J.H.; McClure, M.W.; Horne, R.N. Field observations at the Fenton Hill enhanced geothermal system test site support mixed-mechanism stimulation. *Geothermics* **2018**, *74*, 135–149. [[CrossRef](#)]
13. Brown, D.W.; Duchane, D.V. Scientific progress on the Fenton Hill HDR project since 1983. *Geothermics* **1999**, *28*, 591–601. [[CrossRef](#)]
14. He, R.; Rong, G.; Tan, J.; Phoon, K.; Quan, J. Numerical evaluation of heat extraction performance in enhanced geothermal system considering rough-walled fractures. *Renew. Energy* **2022**, *188*, 524–544. [[CrossRef](#)]
15. Mahmoodpour, S.; Singh, M.; Turan, A.; Bär, K.; Sass, I. Simulations and global sensitivity analysis of the thermo-hydraulic-mechanical processes in a fractured geothermal reservoir. *Energy* **2022**, *247*, 123511. [[CrossRef](#)]
16. Mahmoodpour, S.; Singh, M.; Bär, K.; Sass, I. Thermo-hydro-mechanical modeling of an enhanced geothermal system in a fractured reservoir using carbon dioxide as heat transmission fluid- A sensitivity investigation. *Energy* **2022**, *254*, 124266. [[CrossRef](#)]

17. Zheng, J.; Li, P.; Dou, B.; Fan, T.; Tian, H.; Lai, X. Impact research of well layout schemes and fracture parameters on heat production performance of enhanced geothermal system considering water cooling effect. *Energy* **2022**, *255*, 124496. [[CrossRef](#)]
18. Zhixue, S.; Jiang, C.; Wang, X.; Zhou, W.; Lei, Q. Combined Effects of Thermal Perturbation and In-situ Stress on Heat Transfer in Fractured Geothermal Reservoirs. *Rock Mech. Rock Eng.* **2021**, *54*, 1–17.
19. Liu, J.; Xue, Y.; Zhang, Q.; Wang, H.; Wang, S. Coupled thermo-hydro-mechanical modelling for geothermal doublet system with 3D fractal fracture. *Appl. Therm. Eng.* **2022**, *200*, 117716. [[CrossRef](#)]
20. de Hoop, S.; Voskov, D.V.; Bertotti, G.; Barnhoorn, A. An Advanced Discrete Fracture Methodology for Fast, Robust, and Accurate Simulation of Energy Production From Complex Fracture Networks. *Water Resour. Res.* **2022**, *58*, e2021WR030743. [[CrossRef](#)]
21. Guo, T.; Zhang, Y.; Zhang, W.; Niu, B.; He, J.; Chen, M.; Yu, Y.; Xiao, B.; Xu, R. Numerical simulation of geothermal energy productivity considering the evolution of permeability in various fractures. *Appl. Therm. Eng.* **2022**, *201*, 117756. [[CrossRef](#)]
22. Cao, M.; Hirose, S.; Sharma, M.M. Factors controlling the formation of complex fracture networks in naturally fractured geothermal reservoirs. *J. Petrol. Sci. Eng.* **2022**, *208*, 109642. [[CrossRef](#)]
23. Aliyu, M.D.; Finkbeiner, T.; Chen, H.; Archer, R.A. A three-dimensional investigation of the thermoelastic effect in an enhanced geothermal system reservoir. *Energy* **2022**, 125466. [[CrossRef](#)]
24. Ji, J.; Song, X.; Xu, F.; Song, G.; Shi, Y.; Wang, G.; Song, Z.; Li, S. Effects of variable thermophysical properties of water on the heat extraction of an enhanced geothermal system: A numerical case study. *Appl. Therm. Eng.* **2022**, *217*, 119050. [[CrossRef](#)]
25. Wang, G.; Ma, X.; Song, X.; Li, G. Modeling flow and heat transfer of fractured reservoir: Implications for a multi-fracture enhanced geothermal system. *J. Clean. Prod.* **2022**, *365*, 132708. [[CrossRef](#)]
26. Bataillé, A.; Genthon, P.; Rabinowicz, M.; Fritz, B. Modeling the coupling between free and forced convection in a vertical permeable slot: Implications for the heat production of an Enhanced Geothermal System. *Geothermics* **2006**, *35*, 654–682. [[CrossRef](#)]
27. Zhang, J.; Xie, J. Effect of reservoir's permeability and porosity on the performance of cellular development model for enhanced geothermal system. *Renew. Energy* **2020**, *148*, 824–838. [[CrossRef](#)]
28. Song, G.; Song, X.; Ji, J.; Wu, X.; Li, G.; Xu, F.; Shi, Y.; Wang, G. Evolution of fracture aperture and thermal productivity influenced by chemical reaction in enhanced geothermal system. *Renew. Energy* **2022**, *186*, 126–142. [[CrossRef](#)]
29. Zhang, Y.; Zhang, Y.; Zhou, L.; Lei, Z.; Guo, L.; Zhou, J. Reservoir stimulation design and evaluation of heat exploitation of a two-horizontal-well enhanced geothermal system (EGS) in the Zhacang geothermal field, Northwest China. *Renew. Energy* **2022**, *183*, 330–350. [[CrossRef](#)]
30. Song, G.; Song, X.; Xu, F.; Li, G.; Wang, G.; Ji, J.; Shi, Y. Numerical parametric investigation of thermal extraction from the enhanced geothermal system based on the thermal-hydraulic-chemical coupling model. *J. Clean. Prod.* **2022**, *352*, 131609. [[CrossRef](#)]
31. Zhang, W.; Wang, Z.; Guo, T.; Wang, C.; Li, F.; Qu, Z. The enhanced geothermal system heat mining prediction based on fracture propagation simulation of thermo-hydro-mechanical-damage coupling: Insight from the integrated research of heat mining and supercritical CO₂ fracturing. *Appl. Therm. Eng.* **2022**, *215*, 118919. [[CrossRef](#)]
32. Jiang, F.; Chen, J.; Huang, W.; Luo, L. A three-dimensional transient model for EGS subsurface thermo-hydraulic process. *Energy* **2014**, *72*, 300–310. [[CrossRef](#)]
33. Jiang, F.; Luo, L.; Chen, J. A novel three-dimensional transient model for subsurface heat exchange in enhanced geothermal systems. *Int. Commun. Heat Mass Transf.* **2013**, *41*, 57–62. [[CrossRef](#)]
34. Evans, K. *Enhanced/Engineered Geothermal System: An Introduction with Overviews of Deep Systems Built and Circulated to Date*; China Geothermal Development Forum: Beijing, China, 2010; pp. 395–418.
35. Stephens, J.C.; Jiusto, S. Assessing innovation in emerging energy technologies: Socio-technical dynamics of carbon capture and storage (CCS) and enhanced geothermal systems (EGS) in the USA. *Energy Policy* **2010**, *38*, 2020–2031. [[CrossRef](#)]
36. Aliyu, M.D.; Chen, H. Enhanced geothermal system modelling with multiple pore media: Thermo-hydraulic coupled processes. *Energy* **2018**, *165*, 931–948. [[CrossRef](#)]
37. Zhang, J.; Zhao, M.; Wang, G.; Ma, P. Evaluation of heat extraction performance of multi-well injection enhanced geothermal system. *Appl. Therm. Eng.* **2022**, *201*, 117808. [[CrossRef](#)]
38. Barenblatt, G.; Zheltov, Y.P.; Kochina, I.N. Basic Concepts in the Theory of Seepage of Homogeneous Liquids in Fissured Rocks. *Prikl. Mat. Mekh.* **1960**, *24*, 852–864.
39. WARREN, J.; ROOT, P. The Behavior of Naturally Fractured Reservoirs. *Soc. Pet. Eng. J.* **1963**, *3*, 245–255. [[CrossRef](#)]
40. Gilman, J.; Kazemi, H. Improved Calculations for Viscous and Gravity Displacement in Matrix Blocks in Dual-Porosity Simulators (includes associated papers 17851, 17921, 18017, 18018, 18939, 19038, 19361 and 20174). *J. Pet. Technol.* **1988**, *40*, 60–70. [[CrossRef](#)]
41. Correia, M.G.; Hohendorff Filho, J.C.V.; Schiozer, D.J. Development of a special connection fracture model for reservoir simulation of fractured reservoirs. *J. Pet. Sci. Eng.* **2019**, *183*, 106390. [[CrossRef](#)]
42. Fung, L. Simulation of Block-to-Block Processes in Naturally Fractured Reservoirs. *SPE Reserv. Eng.* **1991**, *6*, 477–484. [[CrossRef](#)]
43. Zeng, Y.; Wu, N.; Su, Z.; Wang, X.; Hu, J. Numerical simulation of heat production potential from hot dry rock by water circulating through a novel single vertical fracture at Desert Peak geothermal field. *Energy* **2013**, *63*, 268–282. [[CrossRef](#)]
44. Hayashi, K.; Willis-Richards, J.; Hopkirk, R.J.; Niibori, Y. Numerical models of HDR geothermal reservoirs—A review of current thinking and progress. *Geothermics* **1999**, *28*, 507–518. [[CrossRef](#)]
45. O'Sullivan, M.J.; Pruess, K.; Lippmann, M.J. State of the art of geothermal reservoir simulation. *Geothermics* **2001**, *30*, 395–429. [[CrossRef](#)]

46. Willis-Richards, J.; Wallroth, T. Approaches to the modelling of hdr reservoirs: A review. *Geothermics* **1995**, *24*, 307–332. [[CrossRef](#)]
47. Pruess, K. Modeling of geothermal reservoirs: Fundamental processes, computer simulation and field applications. *Geothermics* **1990**, *19*, 3–15. [[CrossRef](#)]
48. Li, S.; Feng, X.; Zhang, D.; Tang, H. Coupled thermo-hydro-mechanical analysis of stimulation and production for fractured geothermal reservoirs. *Appl. Energy* **2019**, *247*, 40–59. [[CrossRef](#)]
49. Li, S.; Zhang, D.; Li, X. A New Approach to the Modeling of Hydraulic Fracturing Treatments in Naturally Fractured Reservoirs. *SPE J.* **2017**, *22*, 1064–1081. [[CrossRef](#)]
50. Cao, W.; Huang, W.; Jiang, F. A novel thermal–hydraulic–mechanical model for the enhanced geothermal system heat extraction. *Int. J. Heat Mass Transf.* **2016**, *100*, 661–671. [[CrossRef](#)]
51. Samardzioska, T.; Popov, V. Numerical comparison of the equivalent continuum, non-homogeneous and dual porosity models for flow and transport in fractured porous media. *Adv. Water Resour.* **2005**, *28*, 235–255. [[CrossRef](#)]
52. Asai, P.; Panja, P.; McLennan, J.; Moore, J. Efficient workflow for simulation of multifractured enhanced geothermal systems (EGS). *Renew. Energy* **2019**, *131*, 763–777. [[CrossRef](#)]
53. Gan, Q.; Candela, T.; Wassing, B.; Wasch, L.; Liu, J.; Elsworth, D. The use of supercritical CO₂ in deep geothermal reservoirs as a working fluid: Insights from coupled THMC modeling. *Int. J. Rock Mech. Min. Sci.* **2021**, *147*, 104872. [[CrossRef](#)]
54. Guo, T.; Tang, S.; Sun, J.; Gong, F.; Liu, X.; Qu, Z.; Zhang, W. A coupled thermal-hydraulic-mechanical modeling and evaluation of geothermal extraction in the enhanced geothermal system based on analytic hierarchy process and fuzzy comprehensive evaluation. *Appl. Energy* **2020**, *258*, 113981. [[CrossRef](#)]
55. Cui, G.; Ren, S.; Zhang, L.; Wang, Y.; Zhang, P. Injection of supercritical CO₂ for geothermal exploitation from single- and dual-continuum reservoirs: Heat mining performance and salt precipitation effect. *Geothermics* **2018**, *73*, 48–59. [[CrossRef](#)]
56. Huang, M.; Jiao, Y.; Luo, J.; Yan, C.; Wu, L.; Guan, P. Numerical investigation on heat extraction performance of an enhanced geothermal system with supercritical N₂O as working fluid. *Appl. Therm. Eng.* **2020**, *176*, 115436. [[CrossRef](#)]
57. Asai, P.; Panja, P.; McLennan, J.; Deo, M. Effect of different flow schemes on heat recovery from Enhanced Geothermal Systems (EGS). *Energy* **2019**, *175*, 667–676. [[CrossRef](#)]
58. Guo, T.; Gong, F.; Wang, X.; Lin, Q.; Qu, Z.; Zhang, W. Performance of enhanced geothermal system (EGS) in fractured geothermal reservoirs with CO₂ as working fluid. *Appl. Therm. Eng.* **2019**, *152*, 215–230. [[CrossRef](#)]
59. Zhao, Y.; Zhang, L.; Zhao, J.; Luo, J.; Zhang, B. “Triple porosity” modeling of transient well test and rate decline analysis for multi-fractured horizontal well in shale gas reservoirs. *J. Pet. Sci. Eng.* **2013**, *110*, 253–262. [[CrossRef](#)]
60. Huang, J.; Jin, T.; Chai, Z.; Barrufet, M.; Killough, J. Compositional simulation of fractured shale reservoir with distribution of nanopores using coupled multi-porosity and EDFM method. *J. Pet. Sci. Eng.* **2019**, *179*, 1078–1089. [[CrossRef](#)]
61. Yan, B.; Alfi, M.; Wang, Y.; Killough, J. A New Approach for the Simulation of Fluid Flow in Unconventional Reservoirs through Multiple Permeability Modeling. In *SPE Annual Technical Conference and Exhibition*; OnePetro: Richardson, TX, USA, 2013.
62. Ye, Z.; Qin, H.; Chen, Y.; Fan, Q. An equivalent pipe network model for free surface flow in porous media. *Appl. Math. Model.* **2020**, *87*, 389–403. [[CrossRef](#)]
63. Xu, C.; Fidelibus, C.; Dowd, P.; Wang, Z.; Tian, Z. An iterative procedure for the simulation of the steady-state fluid flow in rock fracture networks. *Eng. Geol.* **2018**, *242*, 160–168. [[CrossRef](#)]
64. Chen, Y.; Ma, G.; Wang, H.; Li, T.; Wang, Y. Application of carbon dioxide as working fluid in geothermal development considering a complex fractured system. *Energy Convers. Manag.* **2019**, *180*, 1055–1067. [[CrossRef](#)]
65. Chen, Y.; Ma, G.; Wang, H.; Li, T. Evaluation of geothermal development in fractured hot dry rock based on three dimensional unified pipe-network method. *Appl. Therm. Eng.* **2018**, *136*, 219–228. [[CrossRef](#)]
66. Chen, Y.; Ma, G.; Wang, H. Heat extraction mechanism in a geothermal reservoir with rough-walled fracture networks. *Int. J. Heat Mass Transf.* **2018**, *126*, 1083–1093. [[CrossRef](#)]
67. Sun, Z.; Zhang, X.; Xu, Y.; Yao, J.; Wang, H.; Lv, S.; Sun, Z.; Huang, Y.; Cai, M.; Huang, X. Numerical simulation of the heat extraction in EGS with thermal-hydraulic-mechanical coupling method based on discrete fractures model. *Energy* **2017**, *120*, 20–33. [[CrossRef](#)]
68. Guo, B.; Fu, P.; Hao, Y.; Peters, C.A.; Carrigan, C.R. Thermal drawdown-induced flow channeling in a single fracture in EGS. *Geothermics* **2016**, *61*, 46–62. [[CrossRef](#)]
69. Shi, Y.; Song, X.; Wang, G.; Li, J.; Geng, L.; Li, X. Numerical study on heat extraction performance of a multilateral-well enhanced geothermal system considering complex hydraulic and natural fractures. *Renew. Energy* **2019**, *141*, 950–963. [[CrossRef](#)]
70. Wassing, B.B.T.; van Wees, J.D.; Fokker, P.A. Coupled continuum modeling of fracture reactivation and induced seismicity during enhanced geothermal operations. *Geothermics* **2014**, *52*, 153–164. [[CrossRef](#)]
71. Gan, Q.; Elsworth, D.; Zhao, Y.; Grippa, A.; Hurst, A. Coupled hydro-mechanical evolution of fracture permeability in sand injectite intrusions. *J. Rock Mech. Geotech. Eng.* **2020**, *12*, 742–751. [[CrossRef](#)]
72. Will, J.; Eckardt, S.; Ranjan, A. Numerical Simulation of Hydraulic Fracturing Process in an Enhanced Geothermal Reservoir Using a Continuum Homogenized Approach. *Procedia Eng.* **2017**, *191*, 821–828. [[CrossRef](#)]
73. Konietzky, H.; Wasantha, P.L.P.; Weber, F. Simulating the Single- and Multi-Stage Hydraulic Fracturing: Some Insights Gleaned from Discontinuum and Continuum Modelling. *Procedia Eng.* **2017**, *191*, 1096–1103. [[CrossRef](#)]
74. Xu, C.; Dowd, P.A.; Tian, Z.F. A simplified coupled hydro-thermal model for enhanced geothermal systems. *Appl. Energy* **2015**, *140*, 135–145. [[CrossRef](#)]

75. Bahrami, B.; Nejati, M.; Ayatollahi, M.R.; Driesner, T. Theory and experiment on true mode II fracturing of rocks. *Eng. Fract. Mech.* **2020**, *240*, 107314. [[CrossRef](#)]
76. Zhang, H.; Shen, Z.; Xu, L.; Gan, L.; Ma, Z.; Wu, Q.; Liu, D. Experimental investigation on hydraulic fracturing in cement mortar with tensile stress. *Eng. Fract. Mech.* **2022**, *259*, 108058. [[CrossRef](#)]
77. Wang, B.; Zhang, Q.; Yao, S.; Zeng, F. A semi-analytical mathematical model for the pressure transient analysis of multiple fractured horizontal well with secondary fractures. *J. Pet. Sci. Eng.* **2022**, *208*, 109444. [[CrossRef](#)]
78. Nguyen, H.T.; Lee, J.H.; Elraies, K.A. A review of PKN-type modeling of hydraulic fractures. *J. Pet. Sci. Eng.* **2020**, *195*, 107607. [[CrossRef](#)]
79. Nordgren, R. Propagation of a Vertical Hydraulic Fracture. *Soc. Pet. Eng. J.* **1972**, *12*, 306–314. [[CrossRef](#)]
80. Geertsma, J.; Klerk, F. A Rapid Method of Predicting Width and Extent of Hydraulically Induced Fractures. *J. Pet. Technol.* **1969**, *21*, 1571–1581. [[CrossRef](#)]
81. Khristianovich, S.A.; Zheltov, Y.P. Formation of Vertical fractures by means of highly viscous liquid. In *4th World Petroleum Congress*; OnePetro: Richardson, TX, USA, 1955; Volume 2, pp. 579–586.
82. Settari, A.; Cleary, M. Development and Testing of a Pseudo-Three-Dimensional Model of Hydraulic Fracture Geometry. *SPE Prod. Eng.* **1982**, *1*, 449–466. [[CrossRef](#)]
83. Li, W.; Frash, L.P.; Lei, Z.; Carey, J.W.; Chau, V.T.; Rougier, E.; Meng, M.; Viswanathan, H.; Karra, S.; Nguyen, H.T.; et al. Investigating poromechanical causes for hydraulic fracture complexity using a 3D coupled hydro-mechanical model. *J. Mech. Phys. Solids* **2022**, *169*, 105062. [[CrossRef](#)]
84. Palmer, I.D.; Carroll, H.B. Numerical Solution for Height and Elongated Hydraulic Fractures. In *Proceedings of the SPE/DOE Low Permeability Gas Reservoirs Symposium*, Denver, Co, USA, 14–16 March 1983.
85. Meyer, B. Design Formulae for 2-D and 3-D Vertical Hydraulic Fractures: Model Comparison and Parametric Studies. In *SPE Unconventional Gas Technology Symposium*; OnePetro: Richardson, TX, USA, 1986.
86. Adachi, J.I.; Detournay, E.; Peirce, A.P. Analysis of the classical pseudo-3D model for hydraulic fracture with equilibrium height growth across stress barriers. *Int. J. Rock Mech. Min. Sci.* **2010**, *47*, 625–639. [[CrossRef](#)]
87. Linkov, A.M.; Markov, N.S. Improved pseudo three-dimensional model for hydraulic fractures under stress contrast. *Int. J. Rock Mech. Min. Sci.* **2020**, *130*, 104316. [[CrossRef](#)]
88. Dontsov, E.V.; Peirce, A.P. An enhanced pseudo-3D model for hydraulic fracturing accounting for viscous height growth, non-local elasticity, and lateral toughness. *Eng. Fract. Mech.* **2015**, *142*, 116–139. [[CrossRef](#)]
89. Yang, Z.; Yi, L.; Li, X.; He, W. Pseudo-three-dimensional numerical model and investigation of multi-cluster fracturing within a stage in a horizontal well. *J. Pet. Sci. Eng.* **2018**, *162*, 190–213. [[CrossRef](#)]
90. Zhao, J.; Chen, X.; Li, Y.; Fu, B. Simulation of simultaneous propagation of multiple hydraulic fractures in horizontal wells. *J. Pet. Sci. Eng.* **2016**, *147*, 788–800. [[CrossRef](#)]
91. Zhao, J.; Chen, X.; Li, Y.; Fu, B.; Xu, W. Numerical simulation of multi-stage fracturing and optimization of perforation in a horizontal well. *Pet. Explor. Dev.* **2017**, *44*, 119–126. [[CrossRef](#)]
92. Li, X.; Yi, L.; Yang, Z. Numerical model and investigation of simultaneous multiple-fracture propagation within a stage in horizontal well. *Environ. Earth Sci.* **2017**, *76*, 273. [[CrossRef](#)]
93. Adachi, J.; Siebrits, E.; Peirce, A.; Desroches, J. Computer simulation of hydraulic fractures. *Int. J. Rock Mech. Min. Sci.* **2007**, *44*, 739–757. [[CrossRef](#)]
94. Alekseenko, O.P.; Vaisman, A.M.; Zazovsky, A.F. A new approach to fracturing test interpretation using the PKN model. *Int. J. Rock Mech. Min. Sci.* **1997**, *34*, 356.e1–356.e13. [[CrossRef](#)]
95. Detournay, E. Propagation Regimes of Fluid-Driven Fractures in Impermeable Rocks. *Int. J. Geomech.* **2004**, *2*, 1277–1288. [[CrossRef](#)]
96. Tsai, V.C.; Rice, J.R. A model for turbulent hydraulic fracture and application to crack propagation at glacier beds. *J. Geophys. Res. Earth Surf.* **2010**, *115*, F3. [[CrossRef](#)]
97. Zhang, X.; Detournay, E.; Jeffrey, R. Propagation of a penny-shaped hydraulic fracture parallel to the free-surface of an elastic half-space. *Int. J. Fract.* **2002**, *115*, 125–158. [[CrossRef](#)]
98. Fu, P.; Johnson, S.; Hao, Y.; Carrigan, C. Fully coupled geomechanics and discrete flow network modeling of hydraulic fracturing for geothermal applications. In *Proceedings of the Thirty-Sixth Workshop on Geothermal Reservoir Engineering*, Stanford, CA, USA, 31 January–2 February 2011.
99. Hofmann, H.; Babadagli, T.; Zimmermann, G. Hot water generation for oil sands processing from enhanced geothermal systems: Process simulation for different hydraulic fracturing scenarios. *Appl. Energy* **2014**, *113*, 524–547. [[CrossRef](#)]
100. Salimzadeh, S.; Paluszny, A.; Nick, H.M.; Zimmerman, R.W. A three-dimensional coupled thermo-hydro-mechanical model for deformable fractured geothermal systems. *Geothermics* **2018**, *71*, 212–224. [[CrossRef](#)]
101. Wang, Y.; Papamichos, E. Thermal effects on fluid flow and hydraulic fracturing from wellbores and cavities in low-permeability formations. *Int. J. Numer. Anal. Methods Geomech.* **1999**, *23*, 1819–1834. [[CrossRef](#)]
102. Lei, Q.; Latham, J.; Tsang, C. The use of discrete fracture networks for modelling coupled geomechanical and hydrological behaviour of fractured rocks. *Comput. Geotech.* **2017**, *85*, 151–176. [[CrossRef](#)]
103. Yang, S.; Chen, M.; Huang, Y.; Jing, H.; Ranjith, P.G. An experimental study on fracture evolution mechanism of a non-persistent jointed rock mass with various anchorage effects by DSCM, AE and X-ray CT observations. *Int. J. Rock Mech. Min. Sci.* **2020**, *134*, 104469. [[CrossRef](#)]

104. Lei, Q.; Wang, X. Tectonic interpretation of the connectivity of a multiscale fracture system in limestone. *Geophys. Res. Lett.* **2016**, *43*, 1551–1558. [[CrossRef](#)]
105. Martel, S.J. Progress in understanding sheeting joints over the past two centuries. *J. Struct. Geol.* **2017**, *94*, 68–86. [[CrossRef](#)]
106. Petit, J.P.; Mattauer, M. Palaeostress superimposition deduced from mesoscale structures in limestone: The Matelles exposure, Languedoc, France. *J. Struct. Geol.* **1995**, *17*, 245–256. [[CrossRef](#)]
107. Paluszny, A.; Matthäi, S.K. Numerical modeling of discrete multi-crack growth applied to pattern formation in geological brittle media. *Int. J. Solids Struct.* **2009**, *46*, 3383–3397. [[CrossRef](#)]
108. Atkinson, B.K. Subcritical crack growth in geological materials. *J. Geophys. Res. Solid Earth* **1984**, *89*, 4077–4114. [[CrossRef](#)]
109. Yin, T.; Chen, Q. Simulation-based investigation on the accuracy of discrete fracture network (DFN) representation. *Comput. Geotech.* **2020**, *121*, 103487. [[CrossRef](#)]
110. Dershowitz, W.S.; Einstein, H.H. Characterizing rock joint geometry with joint system models. *Rock Mech. Rock Eng.* **1988**, *21*, 21–51. [[CrossRef](#)]
111. Billaux, D.; Chiles, J.P.; Hestir, K.; Long, J. Three-dimensional statistical modelling of a fractured rock mass—An example from the Fanay-Augères mine. *Int. J. Rock Mech. Min. Sci. Geomech. Abstr.* **1989**, *26*, 281–299. [[CrossRef](#)]
112. Blum, P.; Mackay, R.; Riley, M.S. Stochastic simulations of regional scale advective transport in fractured rock masses using block upscaled hydro-mechanical rock property data. *J. Hydrol.* **2009**, *369*, 318–325. [[CrossRef](#)]
113. Ma, G.; Li, T.; Wang, Y.; Chen, Y. The equivalent discrete fracture networks based on the correlation index in highly fractured rock masses. *Eng. Geol.* **2019**, *260*, 105228. [[CrossRef](#)]
114. Wang, Y.; Li, T.; Chen, Y.; Ma, G. A three-dimensional thermo-hydro-mechanical coupled model for enhanced geothermal systems (EGS) embedded with discrete fracture networks. *Comput. Methods Appl. Mech. Eng.* **2019**, *356*, 465–489. [[CrossRef](#)]
115. Advani, S.; Lee, T.; Lee, J. Three-Dimensional Modeling of Hydraulic Fractures in Layered Media: Part I—Finite Element Formulations. *J. Energy Resour. Technol.-Trans. Asme* **1990**, *112*, 10–19. [[CrossRef](#)]
116. Chen, Z. Finite element modelling of viscosity-dominated hydraulic fractures. *J. Pet. Sci. Eng.* **2012**, *88–89*, 136–144. [[CrossRef](#)]
117. Vasilyeva, M.; Babaei, M.; Chung, E.T.; Spiridonov, D. Multiscale modeling of heat and mass transfer in fractured media for enhanced geothermal systems applications. *Appl. Math. Model.* **2019**, *67*, 159–178. [[CrossRef](#)]
118. Aliyu, M.D.; Chen, H. Optimum control parameters and long-term productivity of geothermal reservoirs using coupled thermo-hydraulic process modelling. *Renew. Energy* **2017**, *112*, 151–165. [[CrossRef](#)]
119. Liu, S.; Ma, F.; Zhao, H.; Guo, J.; Lu, R.; Feng, X. Numerical analysis on the mechanism of hydraulic fracture behavior in heterogeneous reservoir under the stress perturbation. *J. Nat. Gas. Sci. Eng.* **2020**, *78*, 103277. [[CrossRef](#)]
120. Ghaderi, A.; Taheri-Shakib, J.; Sharif Nik, M.A. The distinct element method (DEM) and the extended finite element method (XFEM) application for analysis of interaction between hydraulic and natural fractures. *J. Pet. Sci. Eng.* **2018**, *171*, 422–430. [[CrossRef](#)]
121. Leonel, E.D.; Venturini, W.S. Non-linear boundary element formulation with tangent operator to analyse crack propagation in quasi-brittle materials. *Eng. Anal. Bound. Elem.* **2010**, *34*, 122–129. [[CrossRef](#)]
122. Leonel, E.D.; Chateaufneuf, A.; Venturini, W.S.; Bressolette, P. Coupled reliability and boundary element model for probabilistic fatigue life assessment in mixed mode crack propagation. *Int. J. Fatigue* **2010**, *32*, 1823–1834. [[CrossRef](#)]
123. Crouch, S. Solution of plane elasticity problems by the displacement discontinuity method. *Int. J. Numer. Meth. Eng.* **1976**, *10*, 301–343. [[CrossRef](#)]
124. Kebir, H.; Roelandt, J.M.; Foulquier, J. A new singular boundary element for crack problems: Application to bolted joints. *Eng. Fract. Mech.* **1999**, *62*, 497–510. [[CrossRef](#)]
125. Kebir, H.; Roelandt, J.M.; Chambon, L. Dual boundary element method modelling of aircraft structural joints with multiple site damage. *Eng. Fract. Mech.* **2006**, *73*, 418–434. [[CrossRef](#)]
126. Leonel, E.D.; Venturini, W.S.; Chateaufneuf, A. A BEM model applied to failure analysis of multi-fractured structures. *Eng. Fail. Anal.* **2011**, *18*, 1538–1549. [[CrossRef](#)]
127. Wang, D.; Dong, Y.; Sun, D.; Yu, B. A three-dimensional numerical study of hydraulic fracturing with degradable diverting materials via CZM-based FEM. *Eng. Fract. Mech.* **2020**, *237*, 107251. [[CrossRef](#)]
128. Sun, W.; Fish, J.; Guo, C. Parallel PD-FEM simulation of dynamic fluid-driven fracture branching in saturated porous media. *Eng. Fract. Mech.* **2022**, *274*, 108782. [[CrossRef](#)]
129. Khoei, A.R.; Vahab, M.; Hirmand, M. An enriched-FEM technique for numerical simulation of interacting discontinuities in naturally fractured porous media. *Comput. Methods Appl. Mech. Eng.* **2018**, *331*, 197–231. [[CrossRef](#)]
130. Vahab, M.; Khoei, A.R.; Khalili, N. An X-FEM technique in modeling hydro-fracture interaction with naturally-cemented faults. *Eng. Fract. Mech.* **2019**, *212*, 269–290. [[CrossRef](#)]
131. Zhou, Y.; Yang, D.; Zhang, X.; Chen, W.; Xia, X. Numerical investigation of the interaction between hydraulic fractures and natural fractures in porous media based on an enriched FEM. *Eng. Fract. Mech.* **2020**, *235*, 107175. [[CrossRef](#)]
132. Huang, L.; Dontsov, E.; Fu, H.; Lei, Y.; Weng, D.; Zhang, F. Hydraulic fracture height growth in layered rocks: Perspective from DEM simulation of different propagation regimes. *Int. J. Solids Struct.* **2022**, *238*, 111395. [[CrossRef](#)]
133. Zeng, J.; Li, H.; Zhang, D. Numerical simulation of proppant transport in hydraulic fracture with the upscaling CFD-DEM method. *J. Nat. Gas. Sci. Eng.* **2016**, *33*, 264–277. [[CrossRef](#)]

134. Jiao, K.; Han, D.; Li, J.; Bai, B.; Gong, L.; Yu, B. A novel LBM-DEM based pore-scale thermal-hydro-mechanical model for the fracture propagation process. *Comput. Geotech.* **2021**, *139*, 104418. [[CrossRef](#)]
135. Zhao, Y.; Li, H.; Zhang, L.; Kang, B. Pressure transient analysis for off-centered fractured vertical wells in arbitrarily shaped gas reservoirs with the BEM. *J. Pet. Sci. Eng.* **2017**, *156*, 167–180. [[CrossRef](#)]
136. Cheng, S.; Zhang, M.; Chen, Z.; Wu, B. Numerical study of simultaneous growth of multiple hydraulic fractures from a horizontal wellbore combining dual boundary element method and finite volume method. *Eng. Anal. Bound. Elem.* **2022**, *139*, 278–292. [[CrossRef](#)]
137. Xu, Y.; Li, X.; Liu, Q.; Yang, S.; Tan, X. A semi-analytical solution of finite-conductivity multi-wing fractured well in naturally fractured reservoirs by boundary element method. *J. Pet. Sci. Eng.* **2021**, *203*, 108584. [[CrossRef](#)]